

# GENERATION AND USAGE OF HIGH VOLTAGE STEEP-FRONT IMPULSES

MARIAN COSTEA, ILEANA BĂRAN, TUDOR LEONIDA

**Key words:** High voltage, Impulse generator, Steep-front impulse, Puncture test, Composite insulator steep-front test.

The generation of high voltage steep-front impulses has always been a concern of researchers in the field of high voltage engineering and electromagnetic compatibility. Obtaining such voltage impulses was imposed by the necessity to simulate real stresses of insulation in electrical installations or electromagnetic disturbances having such characteristics (high altitude nuclear electromagnetic pulse, electrostatic discharges or certain switching operations). For the necessity of electromagnetic immunity tests of civil equipment, the amplitudes of these pulses are usually limited to a few kV, and the circuits that produce them are based on power electronics. However, for insulation tests, they are of the order of hundreds of kV. The paper presents three methods to obtain steep high voltage pulses required for testing high voltage insulations. Their advantages and disadvantages (limitations) are discussed for each of them.

## 1. INTRODUCTION

In the field of high voltage testing, the generation and use of steep-front impulses having large amplitudes (tens or hundreds of kV) become mandatory due to the existence of several industrial tests recommended by different standards, such as puncture test in air on glass and ceramic insulators according to IEC 61211, [1], or steep-front tests for composite insulators stipulated by IEC 62217 standard, [2]. A second use of steep-front impulses was related to the occurrence of new equipment such as gas insulated substations-GIS, [3-5], or gas insulated lines-GIL which produces very fast transients.

In the electromagnetic compatibility field, steep-front transient voltages are used to simulate electrostatic discharges or high altitude electromagnetic pulses.

In recent years, an important number of research studies addressed the generation of high voltages with steep-front and the development of suitable measuring instrumentations and procedures, [6-12]. The paper presents the research conducted in the High Voltage Laboratory of Politehnica University of Bucharest in order to obtain high voltage steep-front impulses, using different solutions.

If the required slope of the impulse is not very high (for example up to 1000 kV/μs), high voltage steep-front impulses can be obtained using the conventional Marx generators. An alternative solution consists in the use of the Marx generator as a basic source, supplemented with some dedicated shaping/peaking circuits, such as sphere gaps or different single stage shaping circuits connected to the basic generator by multiple spark gaps (MSG). Each of these solutions is able to produce output voltages with slopes in the range of 2500 kV/μs...5000 kV/μs or even more. All these methods will be described and documented in the paper.

## 2. ADAPTATION OF A STANDARD IMPULSE GENERATOR TO OBTAIN STEEP-FRONT IMPULSES (UP TO 1000 kV/μs)

The generation of high impulse voltages is based for almost a century on the use of Marx multi-stage generators build with resistors and capacitors. An idealized diagram of the shaping circuit for a single-stage voltage impulse generator is shown in Fig.1.

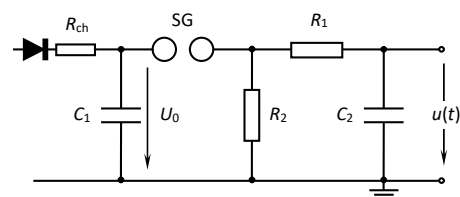


Fig.1 – Basic circuit of a single-stage voltage impulse generator (Marx generator), or schema of the equivalent circuit of a multi-stage impulse voltage generator.

Due to physical dimensions and space disposition of the different constitutive parts, existence of parasitic inductances is inherent. Their actual values depend on a number of factors such as: the generator's construction, its number of stages, the manufacturing technology used for capacitors and resistors. A literature review [13] underscores values from 3 to 5 μH / stage for the internal parasitic inductances. To the internal parasitic inductance, one should add the inductance of the connections to the object under test, whose values depends mainly on their length.

In the absence of the circuit's parasitic inductances, the output voltage has a smooth double-exponential shape, described by the equation (1):

$$u(t) = kU_0 [\exp(-t/\tau_1) - \exp(-t/\tau_2)] \quad (1)$$

where  $U_0$  is the charging voltage,  $k$  a non-dimensional constant,  $\tau_1$  and  $\tau_2$  time constants depending on the main circuit components, namely  $R_1$ -front (or series) resistor,  $R_2$ -tail (or parallel) resistor,  $C_1$ -impulse (or charge) capacitor,  $C_2$ -discharge capacitor. The timing parameters of the output voltage are  $T_1$ -conventional front duration and  $T_2$ -tail duration, both defined in IEC 60060-1 standard. The conventional front duration of the impulse voltage,  $T_1$ , strongly depends on the time constant  $\tau_2$ :

$$\tau_2 = a / \left( b + \sqrt{b^2 - 2a} \right) \ll \tau_1 \quad (2)$$

with  $a = 2R_1R_2C_1C_2$  and  $b = R_1C_1 + R_2C_2 + R_2C_1$ .

The output voltage time derivative given in eq. (3), shows that the average value of the voltage slope on the front of the impulse can be roughly increased operating the generator at high charging voltage per stage ( $U_0$ ) and decreasing the time constant  $\tau_2$ .

$$\frac{du}{dt} = k \frac{U_0}{\tau_2} \left[ -\frac{\tau_2}{\tau_1} \exp(-t/\tau_1) + \exp(-t/\tau_2) \right] \quad (3)$$

A sensitivity analysis shows that the front resistor  $R_1$  value is determinative for the time constant  $\tau_2$  and consequently for  $T_1$ .

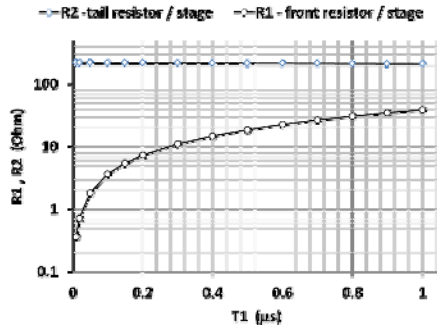


Fig.2 – Front and tail resistors values versus conventional front duration.

As it can be clearly seen from Fig.2, the decrease of  $R_1$  value leads to shorter front durations (considering the capacitances of existent impulse generator described below). If hypothetically we assume a front resistance value of  $R_1 = 0.13 \Omega / \text{stage}$  (giving an overall front resistance of  $2.13 \Omega$  for 6 stages), the front duration equals  $0.01 \mu\text{s}$ . But, an excessive decrease of the  $R_1$  value results in insufficient circuit damping and occurrence of high frequency oscillations due to internal parasitic inductances.

The inductances influence was simulated considering the actual 14 stages Marx generator of the HV Laboratory, with  $C_1 = 0.32 \mu\text{F}/\text{stage}$ ,  $C_2 = 8.96 \text{nF}/\text{stage}$ ,  $R_1 = 7.24 \Omega/\text{stage}$ ,  $R_2 = 217.17 \Omega/\text{stage}$ , combination chose to produce a front time of  $0.20 \mu\text{s}$ . The internal parasitic inductances were assumed to be equal to  $3 \mu\text{H}/\text{stage}$ . The generator was operated with only 6 stages at  $130 \text{kV}/\text{stage}$  charging voltage ( $780 \text{kV}$  total charging voltage). Three cases have been considered and the results are plotted in Fig. 3.

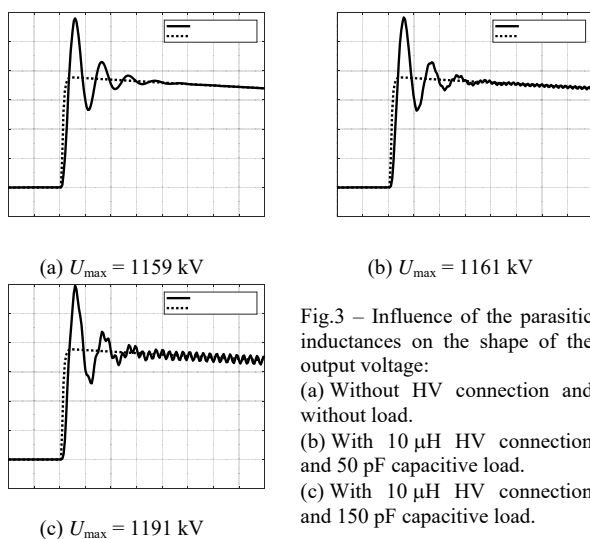


Fig.3 – Influence of the parasitic inductances on the shape of the output voltage:  
 (a) Without HV connection and without load.  
 (b) With  $10 \mu\text{H}$  HV connection and  $50 \text{pF}$  capacitive load.  
 (c) With  $10 \mu\text{H}$  HV connection and  $150 \text{pF}$  capacitive load.

The parasitic inductances, combined with small values of the equivalent capacity of the load, increase the front duration compared to its design value, and generate high frequency damped oscillations superimposed to the double exponential ideal voltage shape.

Therefore, we can conclude that Marx multi-stage generators have intrinsic limitations when set to produce voltage impulses with very fast front and large amplitudes. Limitations have several causes such as:

- the large number of stages required to provide the necessary amplitude of the output voltage, leading to the increase of the overall parasitic inductance,
- the impossibility to reduce, under a recommended threshold, the front resistors' resistance value ( $R_1$ ), a decisive parameter which control the speed of the voltage increase at the generator output terminals,
- the additional dynamic resistance introduced by the generator's spark gaps (SG) when fired,
- difficulties in ensuring synchronous firing of SG (as a large number of stages are necessary).

Another problem related to tests performed with steep-front impulses is the difficulty to measure such fast rising voltages. Because the ratio between the response time of the potential divider and the time to peak of the impulse is responsible, mainly, for the amplitude error of the measured value, potential dividers with very short response time are required. Regarding the transmission systems and the necessary parameters of the measuring device (peak voltmeter, oscilloscope or transient recorder), one can consider that proper solutions should be looked for, capable to meet the demands required by such a signal, since the dynamic performance of all the quoted devices exhibit non-linear deterioration with increasing input signal steepness.

The impulse generator equipping the HV Laboratory was adapted to produce high voltages with average slopes of at least  $1000 \text{kV}/\mu\text{s}$  [14], in order to perform "steep-front test" on composite insulators, according the IEC 62271 standard. Passing over the pre-conditioning of insulators, the test consists in applying a voltage with a slope of at least  $1000 \text{kV}/\mu\text{s}$ , to a  $50 \text{cm}$  segment of the insulator, delimited by two strips of copper firmly attached to the insulator's core, as presented in the Fig.4; it is supposed that the tested insulator length between its metallic fittings exceeds  $50 \text{cm}$ . The gap must be subjected to 25 impulses of both positive and negative polarity with amplitude sufficiently high to produce an external flashover. If no puncture occurs, the insulator passes the test.

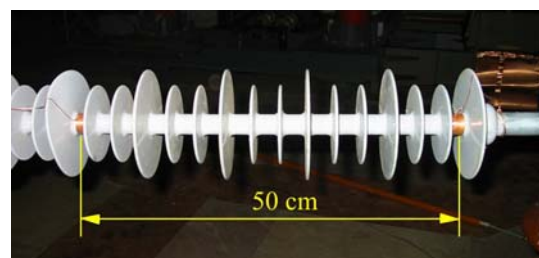


Fig. 4 – Composite insulator for 110 kV rated voltage prepared for steep-front impulse test.

Our goal was to obtain a steep-front impulse using a minimum number of stages and also a minimum charging voltage of the impulse generator. The design value for the (conventional) front time was  $0.7 \mu\text{s}$  instead of  $1.2 \mu\text{s}$  (as for standardized lightning impulse-LI). To lower the front duration to  $0.7 \mu\text{s}$ , the values of series resistors of each stage were reduced at  $2/3$  of the value used to produce the standard  $1.2/50 \mu\text{s}$  LI, while the impulse and charge

capacitors ( $C_1$  and  $C_2$ ) together with the tail resistors ( $R_2$ ) kept the same values as those used for LI.

The measured impulses confirmed the expected results. The impulse generator was operated with 6 stages. The minimum value of the charging voltage required to obtain flashovers as a result of the applied steep-front voltage was 130 kV (the maximum charging voltage of the generator being 250 kV), and the recorded slope of the output voltage was higher than the required 1000 kV/ $\mu$ s value.

The average value of the peak voltage applied during the test procedure was 703 kV with a front time of 0.66  $\mu$ s for negative polarity (leading to 1065 kV/ $\mu$ s average slope), and 712 kV with a front time of 0.68  $\mu$ s for positive polarity (leading to 1047 kV/ $\mu$ s average slope). It is also of interest to mention that the average chopping time was placed around 1  $\mu$ s.

A couple of voltage recordings obtained during these tests is shown in the Fig. 5.

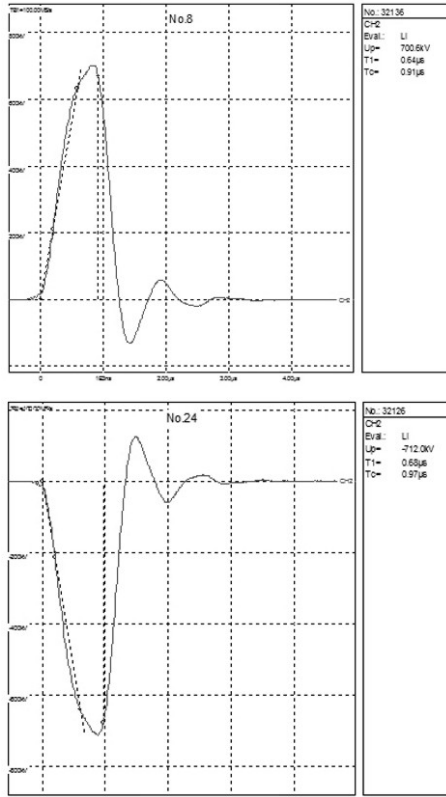


Fig. 5 – Steep-front impulses of positive (a) and negative (b) polarity during tests performed on a composite insulator (110 kV rated voltage).

The approach proves the possibility to perform such a test using a classic voltage impulse generator, the intervention consisting only in reducing the value of the series (front) resistances. Not excessive heating of these resistors has been observed.

### 3. USING RC PEAKING CIRCUIT TO OBTAIN STEEP-FRONT IMPULSES

An alternative solution to obtain HV steep-front impulses is to use a classical impulse generator (IG) as basic voltage source, supplemented with an auxiliary shaping circuit connected to the IG output via a multiple spark-gap (MSG). The peaking circuit is a single stage circuit that can have different schemes; MSG connects IG to the peaking circuit with a very short switching time. An option for the peaking

circuit is represented in Fig. 6: the output of the basic IG is connected to terminals 1 and 2, and the peaking circuit itself is a two-port circuit with the longitudinal branch consisting of the inductance  $L$  in series with the resistor  $R_3$ , and the transversal branch which can be resistive (R), capacitive (C), or a combination (RC). In the HV Laboratory we use the RC transversal branch solution represented in Fig.6; the branch consists of the resistor  $R_d$  in series with the capacitor  $C_d$ . The inductance  $L$  and the resistance  $R_3$  can be intentional circuit's components, or parasitic components of the HV connection between IG and the transversal branch of the peaking circuit.

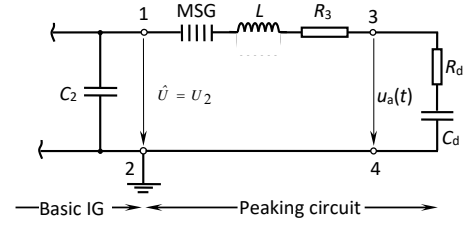


Fig. 6 – A peaking circuit with RC output.

The steep-front impulse voltage provided by the arrangement and applied to the object under test,  $u_a(t)$ , is generated in two stages: (1) following the firing of the IG the voltage between terminals 1 and 2 increases from 0 to the peak voltage  $U_2$ ; (2) if  $U_2$  equals the disruptive voltage set for the MSG, the peaking circuit is connected to the IG through the chain of disruptive discharges which occur inside the MSG, and the output voltage  $u_a(t)$  appears between the terminals 3 and 4. As it was proved in [15], if the MSG switching is instantaneous, then the output voltage  $u_a(t)$  is given by eq. (4):

$$u_a(t) = U_2 \left\{ \frac{C_e}{C_d} \left[ 1 - \frac{1}{\sqrt{1-k^2}} \cdot e^{-\frac{t}{\tau}} \cdot \cos(\omega t - \psi) \right] + \dots \right. \\ \left. \dots + \frac{R_d}{R_e} \cdot \frac{2k}{\sqrt{1-k^2}} \cdot e^{-\frac{t}{\tau}} \cdot \sin \omega t \right\} \quad (4)$$

where:

$R_e = R_3 + R_d$  – equivalent resistance,

$C_e = (C_2 \cdot C_d) / (C_2 + C_d)$  – equivalent capacitance,

$\tau = (2 \cdot L) / R_e$  – damping time constant,

$\omega = \sqrt{1 / (L \cdot C_e) - (R_e / 2 \cdot L)^2}$  – pseudo-angular frequency;

$k = R_e / (2 \sqrt{L / C_e})$  – circuit damping factor;

$\psi = \text{atan}(1 / \omega \cdot \tau) = \text{atan}(k / \sqrt{1 - k^2})$  – phase angle.

The equation (4) is valid if the peaking circuit is under-damped, therefore the damping factor should be in the range  $k \in (0, 1)$ . It is easy to obtain the output voltage for the case of a peaking circuit with pure resistive or capacitive transversal branch from this equation. If  $C_d \rightarrow \infty$  (resistive transversal branch) in eq. (4),  $C_e$  will be replaced by  $C_2$ . If  $R_d = 0$  (capacitive transversal branch) in eq. (4),  $R_e$  will be replaced by  $R_3$ .

In order to compare the three possible options for the transversal branch (namely R, C or RC), a sensitivity study was performed centered to the following parameters of the

output voltage: maximum peak voltage (for a given charging voltage), maximum and average slope, time to reach the maximum slope, and time to crest.

As it was proved, for a given setting of the IG, MSG and the longitudinal peaking circuit's branch, a RC transversal branch has some advantages compared to R or C options: it provides the highest values for the peak voltage and the maximum voltage derivative, as well as the highest peak voltage value for a given intended value of the average slope. Consequently, the RC option has been chosen and a method to design the peaking circuit has been developed. This method is based on the following assumptions: the capacitance  $C_2$  in Fig. 6 is the charge capacitance of the basic IG, the longitudinal branch of the peaking circuit has only the inductance  $L$ , which depends on the length of the HV connection between the IG and the transversal branch  $R_d-C_d$ , the resistance  $R_3$  being neglected.

The design method is based on the following input data:

- *utilization factor* of the peaking circuit,  $c_p = U_p/U_2$ , defined as the ratio between the peak output voltage,  $U_p = \max\{u_a(t)\}$  and the peak input voltage,  $U_2$ ;
- *intended average rise slope*,  $S_{av} = U_p/T_p$ , where  $T_p$  is the time to peak of the output voltage  $u_a(t)$ ;
- *intended peak value* of the output voltage,  $U_p$ .

Accordingly, the design method outputs the following results:

- the values of the circuit elements  $R_d$  and  $C_d$ ;
- the value of the voltage  $U_2$  at the peaking circuit input, required to obtain the desired steep-front impulse parameters (intended peak value and average rise slope defined above).

The utilization factor  $c_p$  should be set close to unity for two reasons: first, if the peaking circuit is under-damped, the overshoot will increase when increasing the value of the utilization factor, and secondly, keeping  $c_p$  close to unity leads to a smooth shape of the steep-front impulse, without oscillations on the impulse's tail.

Our intention was to obtain a steep-front impulse with an average rise slope of about  $5000 \text{ kV}/\mu\text{s}$  using 4 stage of the existing IG with 250 kV maximum charging voltage per stage. The IG was set to produce standard LI. For the following input data:  $C_2 = 2.25 \text{ nF}$  (the equivalent value of the discharge capacitances of the IG operating with 4 stages),  $L = 4 \mu\text{H}$ ,  $U_p = 500 \text{ kV}$ , and choosing an utilization factor equal to 1.0, the evaluation for the output data is  $C_d = 1011 \text{ pF}$ ,  $R_d = 94.7 \Omega$  and a necessary peak value  $U_2 = 505 \text{ kV}$  at the input in the peaking circuit. The shape of the resulting steep-front impulse is plotted in Fig. 7.

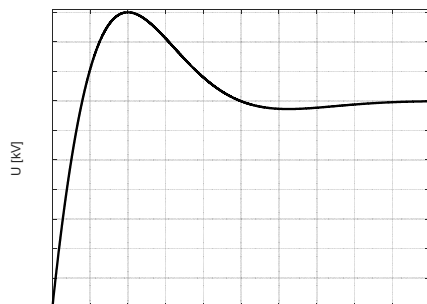


Fig. 7 – Simulated steep-front impulse for  $c_p = 1.0$ .

For a utilization factor  $c_p = 1.1$ ,  $U_p = 500 \text{ kV}$  and  $S_{av} = 5100 \text{ kV}/\mu\text{s}$  average rise slope, the resulting output data are  $C_d = 635 \text{ pF}$ ,  $R_d = 87.2 \Omega$  and  $U_2 = 458 \text{ kV}$ . For practical reasons, a compromise solution was adopted:

a capacitive damped divider with  $C_d = 590 \text{ pF}$  and  $R_d = 290 \Omega$  has been used as transversal branch of the peaking circuit. The reason why such a solution was adopted is related to the difficulty of building HV circuit components at exactly required values and which can withstand, in addition, the electrical stress to which such a transversely installed element will be subjected.

The difference between the design and the actual values results is acceptable for the capacitance  $C_d$  but due to the higher value of  $R_d$ , the peaking circuit will be over-damped.

Even in these conditions, using a self-ignition MSG (10 gaps of 1...3 cm between 11 spheres of 10 cm diameter, in air at atmospheric pressure), we have obtained impulses with time to peak shorter than 100 ns. An example of such a steep-front impulse is given in Fig. 8.

All the tests performed at different charging voltages and different settings of the MSG, have proved the ability of the design method exposed above to provide appropriate estimations for the peaking circuit settings in order to obtain steep-front impulses.

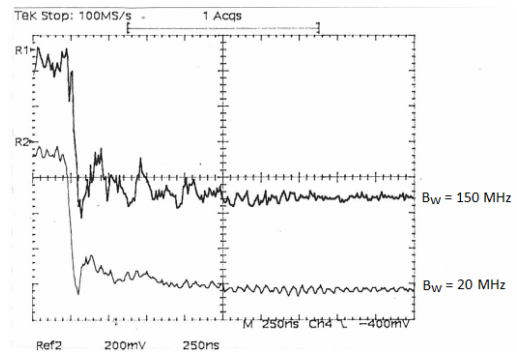


Fig. 8 – Measured negative fast front impulse with 250 kV peak value and 75 ns time to peak.

A second challenge that adds to that of producing a steep front impulse is to measure it. To have a measuring system with fast response, we built a potential divider based on electric field sensor (the high voltage arm was an air gap between two well geometric defined electrodes: sphere-hemisphere), [15]. The  $50 \Omega$  output of the low voltage arm (having R-C structure) was connected to the input of a fiber optic transmission system (of 100 MHz bandwidth, rise time 3.5 ns). The potential divider itself was investigated in order to evaluate the parameters of its step-response, the necessary damping resistor value and the scale factor. This last parameter was determined for an input impulse with the shape  $0.1/50 \mu\text{s}$ . The following parameters have been obtained by processing the step-response of divider: experimental response time,  $T_N = 13.3 \text{ ns}$ , stabilization time,  $t_s = 255 \text{ ns}$  and partial response time,  $T_\alpha = 20 \text{ ns}$ . The scale factor of the divider was 1492. The measuring device was a digital oscilloscope with 150 MHz analogue bandwidth and 100 MSa/s sampling rate.

Comparing the measured and calculated response of the system for a  $0.1/50 \mu\text{s}$  voltage impulse, the amplitude errors did not exceed 5%.

#### 4. USAGE OF SPHERE-GAP AS PEAKING CIRCUIT

Another possibility to obtain a high voltage steep-front impulse is presented in Fig. 9. A sphere-gap ( $SG_2$ ), in series with the tested equipment, is connected to the output terminals of a basic IG. The impulse amplitude depends on the output voltage of the basic IG correlated with the length of the sphere-gap ( $SG_2$ ). In order to obtain a very fast front of the impulse, the spheres diameter and the sparking distance should be set in order to maintain a (practical) homogeneous electric field. In other words,  $SG_2$  should be operated with sparking distances smaller than the sphere radius.

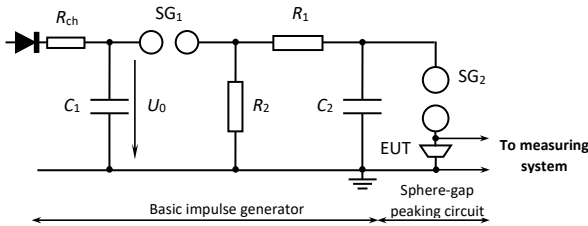


Fig. 9 – Steep front impulse generator based on sphere-gap peaking circuit (EUT- equipment under test).

Generally, this arrangement is used to perform tests on small size insulators, for example tests to check of the puncture voltage in atmospheric air for cap-and-pin insulators.

Our measuring system does not comply entirely with the severe requirements of IEC 61211 (for example, a response time  $\leq 5$  ns and a first partial response time  $\leq 3$  ns for the measuring system without instrument). The instrument (digital recorder) complies partially with the requirements: its rise time is equal to 7 ns and the resolution is of 12 bits. Only the sampling rate (which is of 100 MSa/s) is lower than the recommended one (500 MSa/s). But, even in these conditions, comparative measurements can be performed. As an example, for a triangular shape impulse with the peak time  $T_p$  and a measuring system with monotonic and positive response time,  $T_N$ , the relative amplitude error is  $\delta U = -T_N/T_p$  [15].

For this experiment we have used a 6 stages impulse generator and a maximum charging voltage of 200 kV/stage, operated with only 4 stages. The generator was set to produce standardized lightning impulse (LI) voltage. At the output of the IG we have connected a 200 mm diameter sphere-sphere gap in series with a cap and pin toughened glass insulator. The sparking distance was set at 40 mm and 60 mm respectively, in order to keep a practical homogeneous electric field inside the gap.

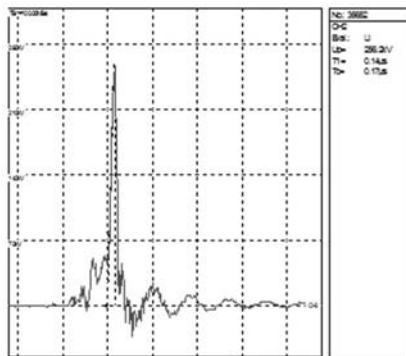


Fig. 10 – Steep-front impulse obtained using a sphere-gap as peaking circuit.

The amplitude of the LI provided by the basic generator has been coordinated with the voltage-time characteristics ( $U_d-T_d$ ) of the sphere gap, in order to locate all the disruptive discharges occurring between the spheres on the front of the LI (100% flashover probability zone of the  $U_d-T_d$  characteristics).

An example of steep-front voltage recorded at the pin terminal of the tested insulator is presented in the Fig. 10; the time parameters have been evaluated following the rules recommended for the LI.

For a charging voltage per stage between 50 kV and 100 kV, the conventional front time do not exceed 200 ns for the sparking distance of 60 mm and 350 ns for the sparking distance of 40 mm. The impulse voltage slope varies between 1000 kV/ $\mu$ s (40 mm sparking distance) to over 1800 kV/ $\mu$ s (60 mm sparking distance) increasing with the increase of the sparking distance, as it has been observed.

From the experiments that have been performed using this solution, some conclusions can be drawn: (1) two impulses with the same crest voltage, but produced using different sparking distances, have practically the same shape; (2) for a set value of the IG charging voltage, the slope increases with the sparking distance, especially due to the amplitude increasing correlated with the decrease of front duration. This effect is illustrated by the comparison between the two chopped impulses shown in the Fig. 11.

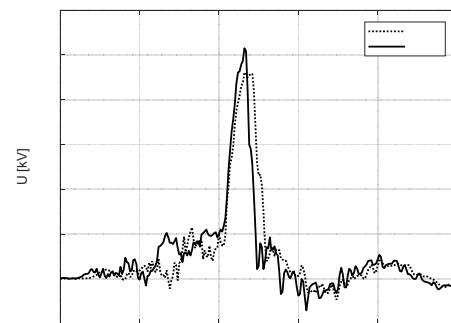


Fig. 11 – Steep-front impulses obtained with the same charging voltage (95 kV) and different lengths for the sphere gap.

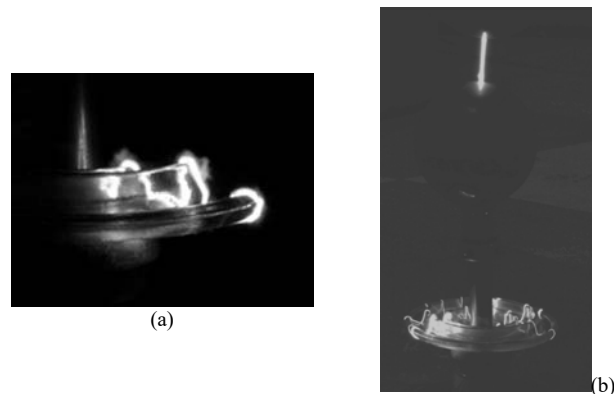


Fig. 12 – Flashover of the cap-and-pin insulator under test while applying (a) standard LI impulse, and (b) steep front impulse.

The impulses which have been obtained using the same charging voltage (95 kV), but with different sparking distances, and applied to a cap-and-pin insulator, have been leading to flashovers that can be seen in Fig. 12. No puncture of the insulator was recorded, but the goal of the experiment did not intend to reach this event.

Generally, such an insulator must withstand, without puncture, a peak voltage equal to 2.5 p.u., the reference being the LI negative flashover voltage of the same tested object.

The comparison of the two steep-front impulses reported in Fig. 11 highlights the followings: the amplitudes of the impulses differs with about 27 kV, the rise time is the same, the slope is higher with about 200 kV/ $\mu$ s for the 60 mm sparking-distance, and the difference between the time to chopping values is about 40 ns, the time to chopping being larger for the sparking distance of 40 cm.

A special mention should be done relative to the differences in the visual aspect of the flashovers in Fig. 12: the flashover under steep-front impulse (Fig. 12.b) exhibits several discharge channels compared to the flashover under standard LI (Fig. 12.a), which signals possible differences induced by the increase of the voltage slope on the mechanism of the discharge development. In the upper part of Fig. 12.b is also visible the discharge between spheres, the picture being taken in dark conditions.

## 5. CONCLUSIONS

The paper presents three possible solutions to obtain steep front impulses based on an existing classical impulse generator (Marx generator): by adapting an existing one by changing the series resistances, by adding at its output a single peaking stage adequately designed and finally by using a sphere gap as peaking circuit.

The first two methods make possible the control of the average slope of the impulse voltage by means of analytical calculations. The last available solution can control the average slope only by experiment, choosing a sphere gap with given diameters and adjusting the distance between spheres in order to obtain the required amplitude of the impulse voltage, correlated with a given time to crest. In this case it would be recommended to establish, with a sufficient number of tests, a table of values useful to avoid a long-lasting probing phase.

## ACKNOWLEDGMENT

The entire experimental tests were performed using the High Voltage Laboratory facilities from Politehnica University

of Bucharest which founder was academician Gleb Drăgan.

Received on April 8, 2020

## REFERENCES

1. \*\*\* *Insulators of ceramic material or glass for overhead lines with a nominal voltage greater than 1000 V - Impulse puncture testing in air*, IEC 61211:2004 Std.
2. \*\*\* *Polymeric HV insulators for indoor and outdoor use – General definitions, test methods and acceptance criteria*, IEC 62217:2012 Std.
3. *Monograph on GIS very fast transients – CIGRE-Brochure no. 35*, July 1989.
4. M. Muhr, S. Pack, *Fast transient overvoltages on a GIS-bushing*, 7<sup>th</sup> Intl. Symp. on High Voltage Engineering (ISH) Dresden, Germany, 1991.
5. W. Boeck, R. Witzman, *Main influences on the fast-transient development in gas-insulated substations*, 5<sup>th</sup> Intl. Symp. on High Voltage Engineering (ISH), Braunschweig, Germany, 1987.
6. T.F. 15.09, *Review of research on nonstandard lightning voltage waves*, IEEE Trans. on Power Delivery, **9**, 4, pp. 1972–1981 (1994).
7. J. Fleszynski, E. Sojda, A. Tyman, K. Koruba, *Steep-front impulse voltage tests of composite insulators*, 13<sup>th</sup> Intl. Symp. on High Voltage Engineering, Delft, Netherlands, 2003.
8. K. Marimuthu, S. Vynatheya, N. Vasudev, P. Raja, *Quality analysis of ceramic insulator under steep front impulse voltage*, 20<sup>th</sup> National Power Systems Conference (NPSC), Tiruchirappalli, India, 2018.
9. K. Wiczorek, J. Fleszyński, *Steep-front impulse voltage in diagnostic studies of composite insulators*, IEEE Transactions on Dielectrics and Electrical Insulation, **23**, 3, pp. 1236–1241 (2016).
10. N. Femia, G. Lupò, C. Petrarca, V. Tucci, M. Vitelli, *Performances of high-voltage glass insulators subjected to fast transient overvoltages*, European Trans. on Electrical Power, **6**, 2, pp. 119–124 (1996).
11. W. Hauschild, E. Lemke, *High-Voltage Test and Measuring Techniques*, 2<sup>nd</sup> ed., Springer, 2019.
12. J. Hlavacek, M. Knenicky, *Very fast high voltage impulse generator*, 19<sup>th</sup> Intl. Scientific Conf. on Electric Power Engineering, Brno, Czech Republic, 2018.
13. N. Hylten-Cavallius, *High voltage laboratory planning*, 2<sup>nd</sup> ed., E. Haefely, Basel, 1988.
14. M. Costea, Ileana Băran, T. Leonida, *Special dielectric tests for composite insulators*, Bul. Inst. Politehnic Iași, **62 (66)**, 1, pp.39–50 (2016).
15. M. Costea, *Research on aspects of extending insulation coordination taking into account very fast overvoltages* (in Romanian), Polytechnic Univ. of Bucharest, doctoral thesis, 1998.